AN EXPERIMENTAL STUDY OF FLOW-INDUCED VIBRATION OF A CANTILEVER IN AXIAL AIR-WATER FLOW

R.W. HARRIS, P.G. HOLLAND

Australian Atomic Energy Commission Research Establishment, Lucas Heights, N.S.W. Australia

SUMMARY

Flow-induced vibrations of a cylindrical cantilever in an axially flowing air/water mixture were measured for a range of volumetric flow rate ratios up to approximately 0.7, for three different constant water mass fluxes of 750, 1 350 and 1 950 kg/m^2/s. The results were obtained for two flow conditions: flow on to the free end of the cantilever ("free-end flow") and directly on to the fixed end (and thence over the free end) ("fixed-end flow").

The effect of four different end shapes on the flow-induced vibration for free-end flow were measured for one water mass flux of 1 270 kg/m^2/s, and for a range of volumetric flow rate ratios up to approximately 0.7. The end shapes investigated were blunt, pyramidal, hemispherical and cusp shaped.

1. Introduction

A previous paper (Harris and Holland [1]) investigated the flow-induced vibration of a simple cantilever for one water flow rate in an air/water mixture at volumetric flow ratios up to 0.3. The purpose of the investigation reported in this paper is to extend the range of measurements and study the effects of changing the water flow rate on the level of vibration. The influence of the shape of the end of the cantilever was thought to have an important effect upon the level of vibration, and this was therefore examined experimentally.

2. Experimental Arrangement

2.1 Basic Experimental Arrangement

The experiment was carried out upon a cantilever-mounted brass rod placed concentrically in a test section having the following characteristics:

(a) The test section was a perspex tube 0.91 m long, 2.54 cm i.d., through which was passed an air-water mixture pre-formed approximately 10 diameters upstream of the test section and passed through a honeycomb flow straightening device to ensure uniform mixing. The whole test section was mounted on an anti-vibration mounting to isolate it from external sources of vibration.

(b) The water was circulated by a centrifugal pump, and the air injected via a porous metal sleeve from the compressed air mains.

(c) The test piece was a brass rod of circular cross section, 0.953 cm dia. and 50.8 cm long, supported rigidly at one end by an aerodynamic support.

The rod was arranged so that the last five centimetres of the free end was screwed on, and four different end shapes were available : blunt, hemispherical, pyramidal and cusp shaped.

2.2 Instrumentation

The water flow rate was measured with a turbine flow meter and the air flow rate with a range of rotameters.

The vibration of the cantilever was measured by two pairs of semiconductor strain gauges mounted on opposite sides of the rod, with the axes joining the two pairs at right angles to each other.

2.3 Analysis of Signals

The strain gauge signals were amplified and fed into both a time domain correlator and a spectrum analyser. The correlator was employed to give a reliable estimate of the mean square (variance) of the strain in the cantilever for a reasonably long averaging time of the order of 2 minutes. The spectrum analyser gave a frequency spectrum which allowed the relative response of the rod at resonance to be determined by measuring the height of the resonance peak.

3. Results and Discussion

3.1 Effect of Mass Flux and Gas Fraction Variations on the Vibration Level

The vibration level of the cantilever was summarised both by measuring the total root mean square of the signal from the strain gauges and by measuring the relative strain

density at a frequency corresponding to the resonance of the rod. As the plane of vibration was found to be random it was satisfactory to employ the output from only one set of the strain gauges. The results of these measurements are shown in figure 1 for the free-end flow and figure 2 for the fixed-end flow. In both cases the end of the rod was blunt. Table I shows the numerical data from which the figures were plotted.

It is interesting to note that in both cases the vibration level increases with increasing gas flow rate ratio β up to the highest values used (about 0.7) at which there is a slight indication that a maximum occurs. The effect of mass flux is such that the vibration level at any specified gas fraction increases roughly linearly with mass flux (an analysis reported later in this paper shows the dependence to be proportional to the mass flux to the power 0.83). These trends were also observed by Cedolin et al. [2].

3.2 Correlation of the Data of these Experiments

Winsbury and Ledwidge [3] indicated that the flow-induced vibration levels in an air/water mixture, may be represented by an equation of the form:

$$S = K\beta^n (1 - \beta) \quad , \qquad (1)$$

where S is the r.m.s. strain, and K and n are constants. Thus, a plot of $S/(1 - \beta)$ versus β using logarithmic scales, should produce a straight line. The results obtained for the total r.m.s. microstrain for both free-end and fixed-end flow are plotted in this form in figure 3. The points in figure 3 do approximate to a straight line, although there appears to be some dependence on the mass flux, so that eq. (1) was modified to read:

$$S = K'\beta^{n'}(1 - \beta)\, G^p \quad , \qquad (2)$$

where K', n' and p are constants and G is the water mass flux. A least squares fit to the data was carried out and yielded the following results for the exponents:

No dependence on mass flux (eq. 1)	$n = 2.01$
Mass flux dependence (eq. 2)	$n' = 2.23$, $p = 0.83$

The fit to the data using eq. (1) is also plotted on figure 3.

It should be noted that an attempt to correlate the data in terms of a two phase Reynolds Number was unsuccessful.

3.3 Effect of End Shape on Vibration for Free-end Flow

The results for the r.m.s. vibration, both total and at the cantilever resonant frequency, as a function of β for a fixed water mass flux of 1 270 kg/m^2/s, are given in figures 4 and 5. The results are also listed in Table II. Only free-end flow was considered as the end shape would be a significant factor for this flow situation. The rod end-shape would not be expected to affect the results for the case of fixed-end flow because the gas void which occurs and is attached to the end of the rod continues downstream and does not extend over the rod.

Several interesting features are apparent from the graph. Contrary to what one might expect, the lowest vibration levels occur for the blunt shape and the highest vibration levels for the cusp shape. A possible explanation for the results is that the blunt shape disturbs the flow to a sufficient extent to cause a flow separation resulting in a decrease in the driving forces, which are associated with the momentum transfer due to the large difference in density between the two phases. The cusp shape appears to interfere with the flow only to a small extent, and hence the driving forces are not significantly modified.

4. Conclusions

For a cantilever-mounted rod placed axially in a flowing two-phase mixture, the vibration amplitude in general increased with both increasing water mass flux and (initially) with increasing volume flow rate ratio, however, there exists some evidence of a maximum in the curve for the higher flow rate ratios. No simple scaling in terms of the homogeneous two-phase Reynold Number to take into account the effect of changing water mass fluxes was apparent. However, the results did approximate to an empirical law of the form $\beta^2(1 - \beta)$.

A study of the effect of end shapes for two-phase flow on to the free end of a cantiliver showed that the lowest vibration levels occurred for the blunt shape, and the highest vibration levels for the cusp shape.

5. Acknowledgements

The authors acknowledge the encouragement of Dr. T.J. Ledwidge. Messrs. C.E. Campbell and E. Clarke assisted both in the construction of the experimental apparatus and the acquisition of data. Messrs. W. Carr and D. McColm arranged for the analysis of the signals arising from the transducers.

6. References

[1] HARRIS, R.W. and HOLLAND, P.G., "Response of a Cylindrical Cantilever to Axial Air Water Flow", Proceedings of the First International Conference on Structural Mechanics in Reactor Technology, Paper E3/6, 1972.

[2] CEDOLIN, L., HASSID, A., ROSSINI, T. and SOLIERI, R., "Vibrations Induced by the Two-phase (GAS + LIQUID) Coolant Flow in the Power Channels of a Pressure Tube Type Nuclear Reactor", Proceedings of the First International Conference on Structural Mechanics in Reactor Technology, Paper E4/5, 1972.

[3] WINSBURY, G.J. and LEDWIDGE, T.J., "An Experimental Study of Vibration of a Cluster of Flexible Hollow Cylinders in Axial Air-Water Flow", Second International Conference on Structural Mechanics in Reactor Technology, Paper D3/1, Berlin, Germany, 10-14 September 1973.

TABLE I

VALUES OF MICROSTRAIN DETERMINED AT THE ROOT OF A BLUNT-ENDED CANTILEVER AT A NUMBER OF VOLUMETRIC FLOW RATE RATIOS

VOLUMETRIC FLOW RATE RATIO β	TOTAL MICROSTRAIN					RELATIVE MICROSTRAIN/Hz AT RESONANCE				
	Fixed-end Flow		Free-end Flow			Fixed-end Flow		Free-end Flow		
	Mass Flux ($kg/m^2/s$)					Mass Flux ($kg/m^2/s$)				
	750	1350	750	1350	1950	750	1350	750	1350	1950
0	560	230	50	72	170	3.1	2.7	1.9	8	13
0.16					190					17
0.21		240		160			19		17	
0.25	170				300	13				24
0.32			200					20		
0.33		500		350			39		36	
0.34					540					56
0.36	300					25				
0.42				470					51	
0.43		730					43			
0.45	440		300			36		32		
0.47					920					75
0.52	550		400			44		40		
0.56		1160	470	920	1000		100	40	97	80
0.58	730					64				
0.65		1000		900			80		84	
0.70			830					72		
0.71		1030					9			
0.78			780					4.5		

TABLE II

VALUES OF MICROSTRAIN DETERMINED AT THE ROOT OF A CANTILEVER OF VARIOUS SHAPES AT THE FREE END IN A MASS FLUX OF 1270 kg/m^2/s PASSING OVER THE FREE END

END SHAPE	Blunt	Pyramidal	Hemi-Spherical	Cusp Shaped	Blunt	Pyramidal	Hemi-Spherical	Cusp Shaped
Volumetric Flow Rate Ratio β	Total Microstrain				Relative Microstrain/Hz at Resonance			
0	62	670	41	47	6.3	4.9	4.3	4.0
0.22	140	210	300	500	6.1	22	26	46
0.34	250	170	430	650	11	30	22	60
0.44	400	520	560	850		55	48	85
0.58	620	800	830	950	44	78	72	81
0.66	900	900	1050	1000	64	88	84	106

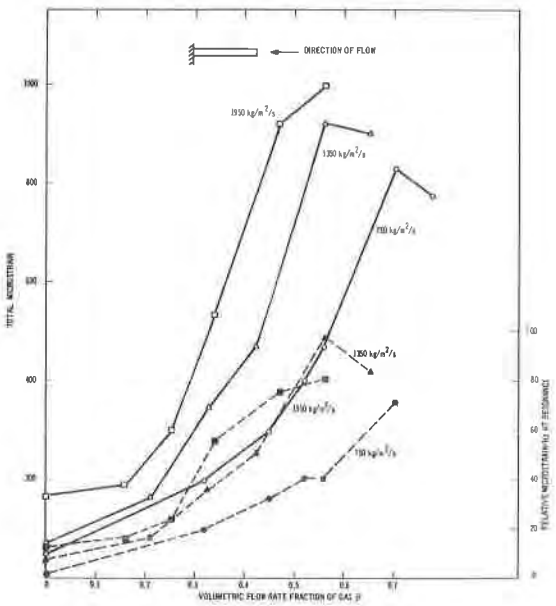

FIGURE 1 R.M.S. STRAIN, BOTH TOTAL (SHOWN BY SOLID LINE) AND RELATIVE PER HERTZ AT RESONANCE (SHOWN BY BROKEN LINE), AS A FUNCTION OF THE GAS FRACTION AND WATER MASS FLUX. (FREE-END FLOW : BLUNT END)

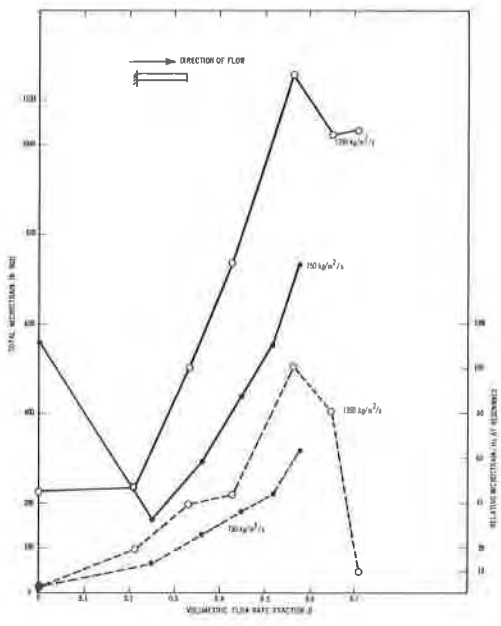

FIGURE 2 R.M.S. STRAIN, BOTH TOTAL (SHOWN BY SOLID LINE) AND RELATIVE PER HERTZ AT RESONANCE (SHOWN BY BROKEN LINE), AS A FUNCTION OF THE GAS FRACTION AND WATER MASS FLUX. (FIXED-END FLOW : BLUNT END)

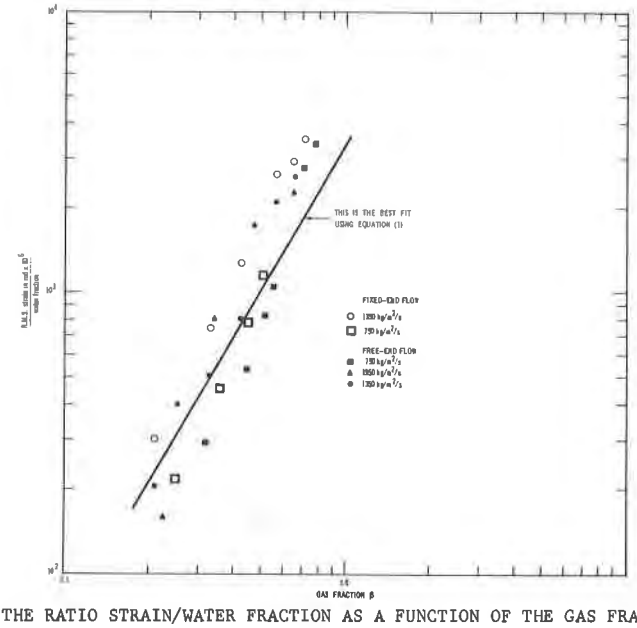

FIGURE 3 THE RATIO STRAIN/WATER FRACTION AS A FUNCTION OF THE GAS FRACTION FOR VARIOUS FLOW CONDITIONS AND WATER MASS FLUXES.

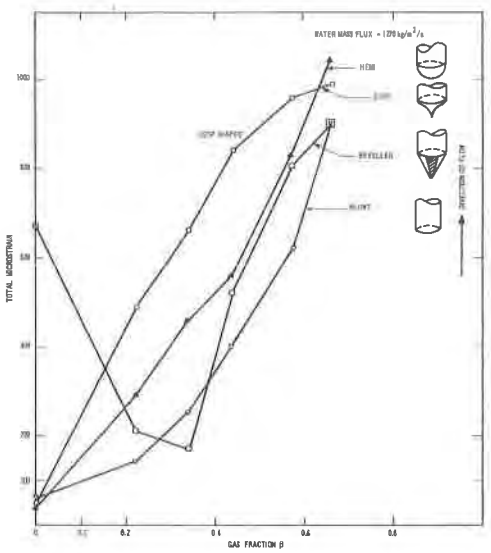

FIGURE 4 TOTAL R.M.S. STRAIN AS A FUNCTION OF THE GAS FRACTION FOR VARIOUS END SHAPES.

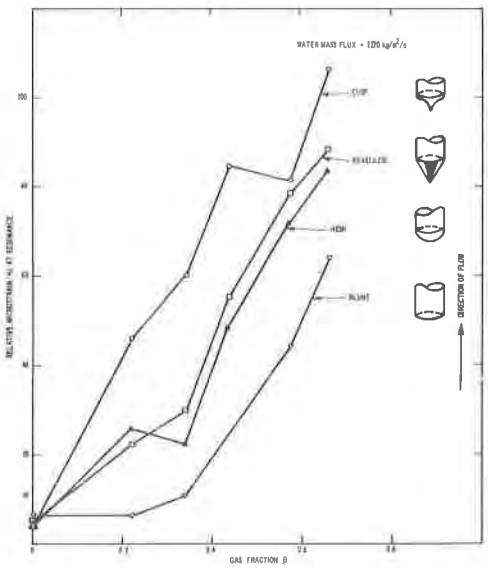

FIGURE 5 RELATIVE STRAIN PER HERTZ AT RESONANCE AS A FUNCTION OF THE GAS FRACTION FOR VARIOUS END SHAPES.